JOURNAL OF MATERIALS SCIENCE **40** (2005) 2281–2286

Atomistic simulations of reactive wetting in metallic systems

E. B. WEBB III, J. J. HOYT, G. S. GREST, D. R. HEINE
Sandia National Laboratories, Albuquerque, NM 87185

Atomistic simulations were performed to investigate high temperature wetting phenomena for metals. A sessile drop configuration was modeled for two systems: Ag(l) on Cu and Pb(l) on Cu. The former case is an eutectic binary and the wetting kinetics were greatly enhanced by the presence of aggressive interdiffusion between Ag and Cu. Wetting kinetics were directly dependent upon dissolution kinetics. The dissolution rate was nearly identical for Ag(l) on Cu(100) compared to Cu(111); as such, the spreading rate was very similar on both surfaces. Pb and Cu are bulk immiscible so spreading of Pb(l) on Cu occurred in the absence of significant substrate dissolution. For Pb(l) on Cu(111) a precursor wetting film of atomic thickness emerged from the partially wetting liquid drop and rapidly covered the surface. For Pb(l) on Cu(100), a foot was also observed to emerge from a partially wetting drop; however, spreading kinetics were dramatically slower for Pb(l) on Cu(100) than on Cu(111). For the former, a surface alloying reaction was observed to occur as the liquid wet the surface. The alloying reaction was associated with dramatically decreased wetting kinetics on Cu(100) versus Cu(111), where no alloying was observed. These two cases demonstrate markedly different atomistic mechanisms of wetting where, for Ag(l) on Cu, the dissolution reaction is associated with increased wetting kinetics while, for Pb(l) on Cu, the surface alloying reaction is associated with decreased wetting kinetics.

1. Introduction

Wetting of liquids on solids is well described by the contact angle θ adopted by a liquid drop. For wetting on inert substrates, θ is determined by establishing a balance between the solid/liquid, liquid/vapor, and solid/vapor surface tensions, as represented by the Young equation [1]. In the two hundred years since this seminal work, much experiment and theory has been applied to understanding wetting and spreading on inert substrates. Prior work has examined contact angles, kinetics of spreading, and spreading morphology such as precursor films, which sometimes are observed to advance diffusively ahead of spreading drops [2–12]. Wetting in metal and metal/oxide systems, important in joining processes like brazing, is often accompanied by reactions between the liquid and the solid. The introduction of reactions to wetting and spreading complicates theoretical descriptions as surface tensions no longer remain constant. Reactions may produce a thin film of product at the solid/liquid interface different from any of the starting constituents [13, 14]. Alternatively, aggressive interdiffusion may occur between the solid and liquid during spreading [15]. Generally, it is observed that reactions increase wettability. One reason for this is that the reaction product formed at the solid/liquid interface can exhibit different interfacial energy than the unreacted substrate. Another factor increasing wettability is the free energy gain of the reaction creating an additional driving force for wetting [16]. Improving wettability via reactions is a fundamental concept for joining metals with metals or oxides via braze and solder processes [17].

Wetting kinetics can be characterized by the radius of the spreading drop as a function of time $R(t)$. Data from experiments and models are typically analyzed to establish power law relations $R(t) \sim t^{\alpha}$, where α is reflective of the assumed driving and resistance forces for wetting. For reactive wetting, a range of behaviors—expressed by different values of α—have been predicted and observed. Some experiments corroborate model predictions but discrepancies exist; excellent examples of this have recently been reviewed, along with chemical complexities associated with reactive wetting [16]. From a theoretical standpoint, some reactive wetting models assume the formation of a thin, wettable reaction product with minimal reaction occurring behind the contact line. These models predict two regimes: for diffusion controlled wetting, $\alpha = 1/4$ [18] whereas for reaction controlled wetting, $\alpha = 1$ [13]. Other models combine reaction and diffusion control, giving regimes with linear ($\alpha = 1$) and non-linear, or decreasing rate, kinetics ($\alpha < 1$) [19, 20]. Which behavior dominates for a given system or for a given range in time is determined by the reactant diffusivity compared to the corresponding reaction rate. Models have also been advanced which relax the assumption of no reaction behind the contact line, resulting in similar kinetics to what is observed for combined

models [15, 20]. Numerical simulations of dissolutive reactive wetting exhibited a decreasing spreading rate [21]. Since most reactive wetting systems are partially wetting and the spreading rate goes to zero at finite θ, it is generally agreed that no single power law can capture all of the phenomena exhibited by these systems [13, 19]. Analytical models, continuum simulation, and interpretation of experimental data can all benefit from a more fundamental description of wetting in reactive systems. One method to achieve this is atomistic simulation such as molecular dynamics (MD).

Atomistic simulations of wetting in metal systems have been performed, but in most of these, reaction between the spreading liquid and the substrate did not occur [22–24]. Some MD simulations of reactive wetting in metal systems have been published by the current authors [25–27]. This prior work is expanded upon here, where wetting of spherical drops of Ag(l) and Pb(l) on both Cu(100) and Cu(111) are compared. Significant differences are demonstrated to exist for these two binary systems. In the following section, the interatomic interaction model and simulation methodology are presented. Results for Ag(l) spreading on Cu are presented in Section 3.1 and for Pb(l) on Cu in Section 3.2 Our conclusions are summarized in Section 4.

2. Model and methodology

MD simulations used the embedded atom method (EAM) to describe interactions between atoms; the EAM employs a multibody interaction to describe bonding and has been widely used in performing atomistic simulations of metals [28–30]. EAM interatomic potential functions are typically fit to existing experimental data, *ab initio* simulation results, or a combination of the two. The details of this model can be found in the references [28–30] and will not be reviewed further here. Foiles *et al.* [29] developed potentials for pure Ag, pure Cu, and the AgCu binary. These potentials predict melting points $T_{\mathrm{m}}^{\mathrm{Ag}} = 1144$ K and $T_{\mathrm{m}}^{\mathrm{Cu}} = 1279$ K compared to experimental results $T_{\mathrm{m}}^{\mathrm{Ag}} = 1234$ K and $T_{\mathrm{m}}^{\mathrm{Cu}} = 1353$ K [27, 31]. Liquidus and solidus phase boundaries were calculated for this model and demonstrated eutectic behavior in good agreement with experiment [27]. Lim *et al.* [32] developed an EAM potential for pure Pb that predicts $T_{\mathrm{m}}^{\mathrm{Pb}} = 618$ K (experiment, $T_{\mathrm{m}}^{\mathrm{Pb}} = 620$ K). Hoyt *et al.* [31] developed an interaction between Pb, as described by the Lim *et al.* potential, and Cu, as described by the Foiles *et al.* potential. Phase boundaries were calculated for PbCu and the model predicted significant immiscibility between Pb and Cu in both the solid and liquid state [31], which agrees well with experiment. While more quantitatively accurate models for AgCu and PbCu could be produced using a more detailed interatomic potential fitting procedure, the models used here are sufficient for making realistic comparisons between wetting in an eutectic metal system to wetting in an immiscible metal system.

Details of simulation procedures have been presented previously [25, 26] so only a brief summary is provided here. FCC Cu crystals were constructed with the [111] or [100] direction oriented along the z axis of the simulation cell. The lattice constant for each temperature T of interest was determined from separate simulations in constant number, pressure, and temperature *NPT* ensembles. $T = 1200$ and 700 K were chosen for simulating wetting in the AgCu and PbCu systems, respectively. In both cases, T investigated is ∼5 to 10% greater than T_{m} for the corresponding liquid but below $T_{\mathrm{m}}^{\mathrm{Cu}}$. After constructing the Cu crystals, subsequent calculations were done holding the cell dimensions in the x and y directions constant with periodic boundary conditions applied in x and y. Open boundary conditions were applied in z, thereby forming two free crystal surfaces. A slab of atoms at one surface was held rigid throughout the simulations while the remaining atoms in the substrate were allowed to relax. The thickness in z of the frozen slab was twice the cutoff for Cu-Cu interactions ($R_c^{\mathrm{Cu}} = 4.95$ Å). The (111) and (100) surface slabs were equilibrated at constant T.

Separately, liquids of Ag and Pb were equilibrated at $T = 1200$ K and 700 K, respectively, in NPT ensemble simulations. Spheres with initial radius R_0 were cut out of each liquid and equilibrated in free space. An equilibrated liquid drop was inserted into a simulation cell just above an equilibrated Cu surface for each of the four cases studied. The initial separation distance between drop and substrate was chosen to correspond with the minimum energy separation distance in the Pb-Cu interaction potential. For simulations using spherical drop starting states, $R_0 = 50$ Å and the dimensions of the simulation cell (130 Å × 130 Å) were such that spreading could be followed for $R(t)$ up to ∼2.5 R_0. For Pb(l) on Cu, wetting behavior was also studied using hemispherical drops as the starting state since substrate dissolution was minimal in this system. In this case, the hemisphere was removed from the liquid simulation cell and joined directly with the corresponding substrate, not permitting any shape relaxation in free space. After joining liquid and solid, all subsequent calculations were done in a canonical NVT ensemble. In all simulations, T was maintained using a Nose-Hoover thermostat algorithm [33] and the simulation timestep was 0.001 ps.

To determine the radius of a spreading drop $R(t)$, slabs were defined in the simulation cell parallel to the Cu surface. For analyzing AgCu results, the thickness in z for each slab was equal to the Cu planar spacing (1.9 Å). For PbCu simulations, a slightly larger thickness was used to account for the relatively large atomic radius of Pb atoms. The slab containing the surface Cu plane at $t = 0$ was designated $l = -1$ and slabs containing atomic planes successively deeper into the crystal were $l = -2$, -3, etc. Similarly, slabs were defined above the Cu surface designated $l = 1$, 2, 3, etc. Within each slab at a given t, the density of drop atoms was calculated as a function of distance from the slab center of mass. These density data were integrated until 98% of drop atoms in the slab were accounted for; the distance at which this occurred was $R(t)$ for the slab.

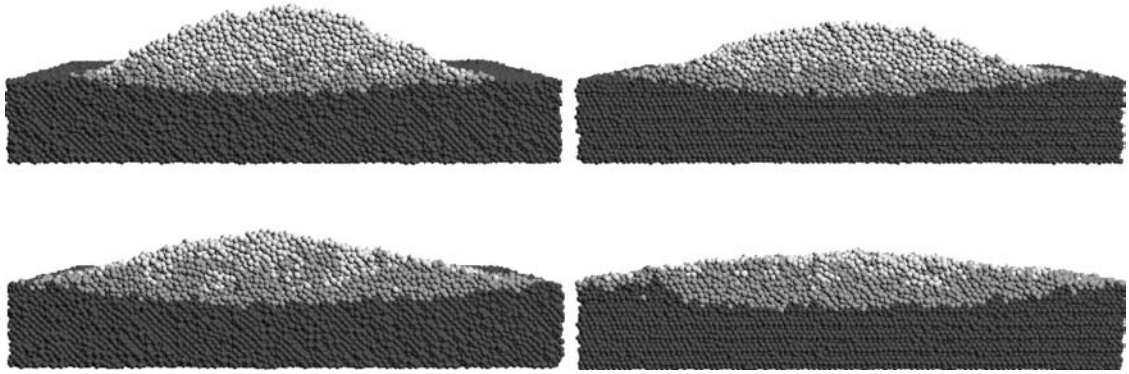

Figure 1 Cross-section snapshots from the simulations of a Ag(l) spherical drop at $T = 1200$ K on Cu(100) (left) and Cu(111) (right). Images are shown for (top) $t = 300$ ps and (bottom) $t = 600$ ps [37]. Non-alloyed Ag(Cu) atoms are white(dark grey); alloyed atoms are light grey. A Ag(Cu) atom is considered alloyed if at least three Cu(Ag) atoms are in its first neighbor shell.

3. Results and discussion

3.1. Ag(l) on Cu

In Fig. 1, cross section snapshots from the simulations of Ag(l) spreading on Cu(100) and Cu(111) are presented. Images are presented after the drops have spread $\sim$100 and $\sim$ 130 Å (i.e. to the edge of the simulation cell). Due to periodic boundary conditions, drop images begin to interact when the drop spreads to the cell boundary so this is when the simulations are ended. To better illustrate the substrate dissolution that occurs during spreading, atoms are colored differently if they are designated as alloyed. This occurs when a given atom gets three or more atoms of the opposite type in its first neighbor sphere. This definition, while arbitrary, is useful for illustrating mixing between Ag and Cu. As seen in Fig. 1, aggressive substrate dissolution occurs for spreading on both crystal surfaces. Prior work compared spreading of Ag(l) on Cu(100) for mobile and rigid substrate lattices [25, 27]. Therein, spreading kinetics were more rapid and total area of spread was greater for the case when substrate dissolution was permitted compared to spreading on a rigid lattice where no mixing was permitted. It was also shown that, as dissolution kinetics decreased, so too did spreading kinetics [27]. The current results indicate that, when substrate dissolution occurs, crystal orientation does little to alter observed wetting behavior. This is exemplified in Fig. 1 by the similarity between snapshots for spreading on Cu(100) compared to Cu(111).

This is further demonstrated in Fig. 2a where we present $R(t)$ for spreading of Ag(l) on Cu(100) and Cu(111). As discussed in Section 2, $R(t)$ was calculated for different slabs parallel to the substrate surface. Data from slabs closest to the solid/liquid interface (i.e., slabs $l = 1$ and -1) essentially overlapped. As such, these data were averaged for each system to produce the curves in Fig. 2a. Both systems exhibit a short early t regime during which the spherical drop rapidly transforms to a hemispherical cap with $\theta < 90^\circ$. Substrate dissolution occurs even during this very rapid spreading stage so the description of hemispherical cap is approximate. This is followed by a regime of slower kinetics wherein spreading rate continues to decrease. While spreading on Cu(111) appears to be somewhat more rapid during the transition to a hemispherical cap,

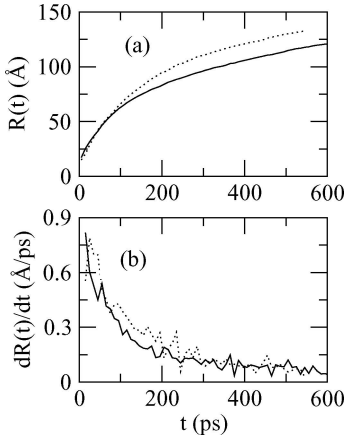

Figure 2 (a) $R(t)$ for wetting of a Ag(l) spherical drop on Cu(100) (solid) and Cu(111) (dashed) at $T = 1200$ K. (b) $dR(t)/dt$ for the same systems.

data after this transition indicate spreading rate is very similar for Ag(l) on Cu(100) and Cu(111). From $R(t)$ in Fig. 2a, instantaneous spreading rate $dR(t)/dt$ was calculated and is presented in Fig. 2b. This further bears out the observations made. The implication is that dissolution rate, which dominates spreading kinetics, is similar for both substrates. In simulations this can be monitored directly by calculating the number of Cu atoms which have dissolved into the liquid as a function of time. This analysis confirmed that the dissolution rate was nearly identical for both crystal orientations throughout the timeframe of the simulations. Fig. 2b indicates that the spreading rate continues to decrease with time throughout the simulation and this, too, corresponds to an observed decrease in dissolution kinetics as the simulations progress; that is, as the liquid becomes more Cu-rich.

The slight increase in kinetics seen at early t on Cu(111) is understandable as this appears to be a surface diffusion limited regime and diffusion of Ag adatoms on Cu(111) is more rapid than on Cu(100). Quickly, though, the dissolution kinetics dominate the spreading kinetics. In this regime the spreading rate for the two substrates is similar because the dissolution rate is similar. Similar dissolution behavior on the different crystal surfaces is of note. The binding energy for Cu atoms at the (111) surface is greater than for atoms at the (100) surface so one might anticipate that dissolution

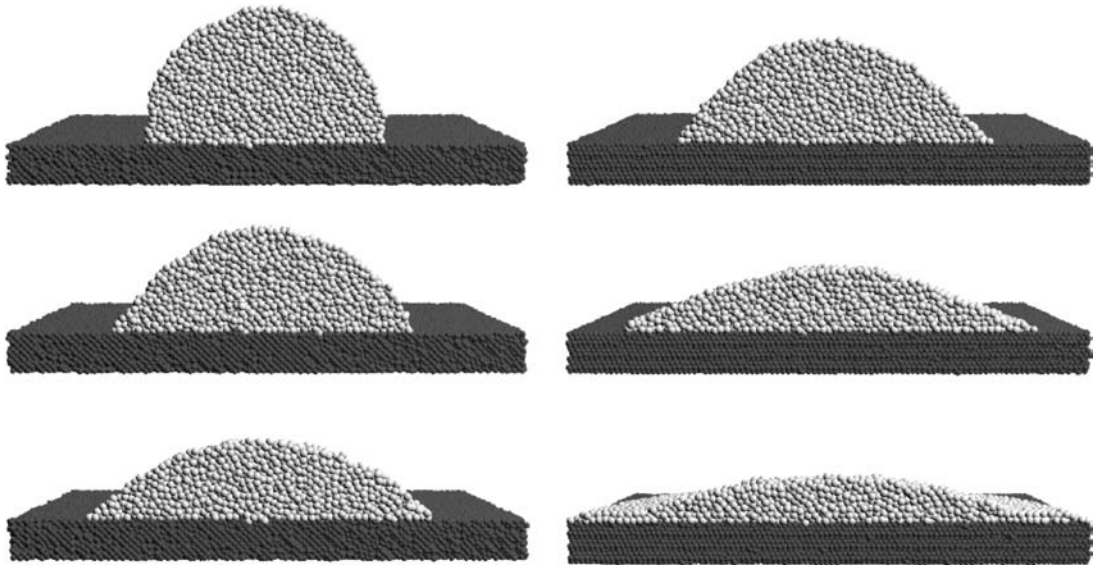

Figure 3 Cross-section snapshots from the simulations of a Pb(l) spherical drop at $T = 700$ K on Cu(100) (left) and Cu(111) (right). Images are shown for (top) $t = 100$ ps, (middle) $t = 200$ ps, and (bottom) $t = 400$ ps. Pb (Cu) atoms are white (dark grey).

kinetics on the former would be slower. Results indicate that binding energy differences do not influence dissolution. This can be explained by noting that dissolution is a collective process that does not depend upon subtle differences in the energy to remove a single atom from the surface. Furthermore, planarity at the solid/liquid interface is clearly disrupted (see Fig. 1). As such, the crystal plane of the surface at $t = 0$ becomes less influential with time since dissolution occurs across the increasingly less planar solid/liquid interface. Substrate dissolution increases the driving force for spreading to a degree related to the free energy change associated with the dissolution reaction. Since this depends upon the concentration of Cu in the liquid, the substrate crystal orientation has little effect on the kinetics. Similar results were found experimentally for dissolutive wetting of Sn on Bi [34].

3.2. Pb(l) on Cu

The bulk binary phase diagram for the PbCu EAM model exhibits, in agreement with experiment, significant regions of immiscibility, even in the liquid state [31]. Correspondingly, virtually no substrate dissolution occurs during the spreading, as illustrated in Fig. 3. Snapshots from simulations of Pb(l) spreading on Cu(100) and Cu(111) are shown. Fig. 3 shows the solid/liquid interface in both systems remains quite planar, in dramatic contrast to the dissolutive wetting displayed for Ag(l) on Cu in Fig. 1. While the PbCu simulations were performed at $T = 700$ K and the AgCu simulations at $T = 1200$ K, the significant difference in substrate response during spreading has little to do with differences in T. The differences exist due to the chemical nature of the systems: AgCu is eutectic whereas PbCu exhibits strong immiscibility. These bulk system properties are directly reflected in interface properties, as exhibited by the wetting behavior.

Fig. 3 shows another distinction from Fig. 1. Results in Fig. 3 for spreading of Pb(l) on Cu(100) are much different than on Cu(111) whereas for Ag(l) spreading on Cu (Fig. 1), there was little dependence upon crystal orientation. For Pb(l) on Cu(111) a precursor film, two atomic layers thick, emerges from the spreading drop and advances rapidly across the substrate, reaching the simulation cell edge $R(t) \sim 2.5R_0$ in a few hundred ps. Results for Pb(l) on Cu(100) are much different in that no precursor film emerges in the time depicted and wetting kinetics are significantly slower. In addtion to spherical droplets, we also carried out simulations using hemispherical starting states in order to study larger droplets [26]. Data from [26] is reproduced in Fig. 4 where we present $R(t)$ for various layers of Pb(l) above the Cu(100) and Cu(111) surface for hemispherical drops of initial radius $R_0 = 100$ Å. Qualitatively, we found from images such as those shown in Fig. 3 for spherical starting states and similar data for hemispheres that using hemispherical starting states does not alter observed wetting behavior. Because the liquid volume is different for the two starting geometries, a quantitative comparison reveals small differences in kinetics but qualitatively identical behavior.

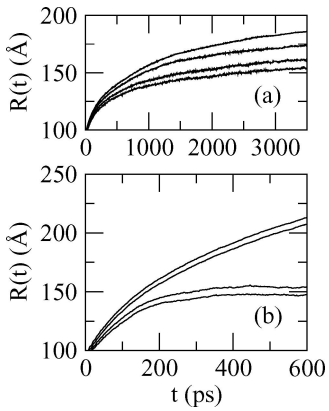

Figure 4 $R(t)$ for wetting of a Pb(l) hemispherical drop on (a) Cu(100) and (b) Cu(111) at $T = 700$ K. Data are shown from different analysis slabs above the Cu surface $l = 1$ to 4 (top to bottom curve on each figure).

For Pb(l) on Cu(111) as shown in Fig. 4, $R(t)$ in layers $l = 1$ and 2 increases significantly faster than in layers $l > 2$. This is the precursor film emerging and Fig. 4 verifies it is two atomic layers thick. For Pb(l) on Cu(100) $R(t)$ data from all layers remains bunched more tightly together until late in t. After ~3000 ps, a foot is seen to emerge from the partially wetting drop and continue to advance ahead of the drop.

Data for the precursor layers on Cu(111) are well described by $R(t) \sim t^{1/2}$ [26]. This was true on Cu(100) as well but not until the foot distinguished itself from the partially wetting drop (i.e. at late t). Wetting kinetics for Pb(l) on Cu(100) are significantly slower than on Cu(111). Analysis of the solid/liquid interface demonstrated that, for the system exhibiting slower wetting kinetics, a disordered surface alloy formed between Pb and Cu as Pb(l) spread on the surface. For Pb(l) wetting Cu(111), no alloy formation was observed during the spreading simulations. That is, the precursor film which rapidly covered the Cu(111) surface was an overlayer of Pb. Wetting simulations were repeated [26] but on substrates that were pre-wet with the appropriate two-layer film: on Cu(100) the surface alloy phase was constructed in the prewet film and on Cu(111) the surface overlayer phase was constructed. Simulating wetting on pre-wet substrates removed the influence of precursor foot kinetics on drop kinetics and the two drops spread at comparable rates. The kinetics of Pb(l) wetting both pre-wet surfaces were well described via the molecular kinetic model [6, 7, 26]. Most notably, kinetics of Pb(l) drops spreading on pre-wet Cu(100) were faster than on bare Cu(100), a clear indication that drop kinetics on the bare surface were limited by slow precursor foot kinetics.

For Pb(l) spreading on the bare Cu(100) substrate, it is observed that the layer of Pb(l) closest to the Cu surface advances over initially pure Cu. Before further advancement, Pb atoms in the $l = 1$ layer exchange with Cu atoms in the surface plane. That is, before foot advancement, a surface alloying reaction occurs between the liquid film and the solid substrate. Furthermore, it has been established that the wetting kinetics of the droplet on bare Cu(100) are controlled by the wetting kinetics of the precursor film. In some models of reactive wetting, a thin layer of wettable reaction product is assumed to form at the solid/liquid interface. The liquid will not wet the bare substrate well but does wet the reaction product [13, 18]. In these models, if formation of the wettable layer is limited by reaction rate at the contact line, linear wetting kinetics are predicted ($R(t) \sim t$) [13, 35]. If reaction product formation is limited by reactant diffusivity to the contact line, models predict $R(t) \sim t^{1/4}$ [18, 36]. A precursor film, two atomic layers thick, is not what is typically implied by a thin film of reaction product. Nonetheless, the system examined here obeys many of the approximations made in arriving at the reaction and diffusion controlled models of reactive wetting. That is, the precursor film reacts with the substrate to form a binary alloy different from either the substrate or the droplet (i.e., a reaction product) and the droplet contact line advances on top of this. Given these similarities, it is interesting to examine the kinetics of the droplet spreading on bare Cu(100) where precursor reaction kinetics seem to be linked to wetting kinetics.

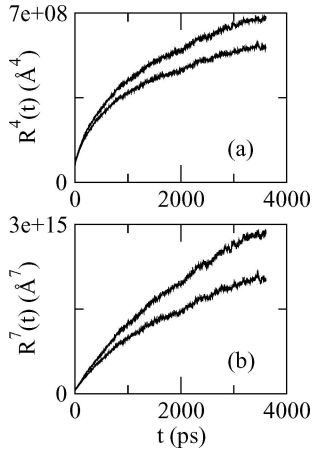

Figure 5 Kinetics of the precursor controlled drop. (a) $R^4(t)$ from layers $l = 3$ (top curve) and 4 (bottom curve) for wetting of a Pb(l) hemispherical drop on Cu(100) at $T = 700$ K. (b) $R^7(t)$ for the same data.

Because the onset radius and time for the kinetic regime of interest are not known precisely, logarithmic plots of the data are of limited utility in revealing power law exponents from the slope in the data. Instead, we plot various powers of $R(t)$ and look for linearity in the data as this can be interpreted as demonstration of a given power law. Data for $l = 3$ and 4 illustrate drop kinetics and in Fig. 4 these curves exhibit negative curvature when plotted linearly. This indicates a decreasing rate of spreading and a departure from predictions of the reaction limited model for reactive wetting. In Fig. 5, $R^4(t)$ and $R^7(t)$ are presented for $l = 3$ and 4 on bare Cu(100). The $R^4(t)$ plot shows negative curvature; thus, data are not well described by the diffusion limited model of reactive wetting. This is not a surprising result since the liquid composition is pure and reactant atoms (Pb) are readily supplied to the contact line throughout spreading. In Fig. 5, the $R^7(t)$ data show a range of reasonable linearity. This indicates that, despite the limit on spreading rate imposed by slow precursor film advancement, Pb(l) drop advancement can be described reasonably well by the molecular kinetic model ($R(t) \sim t^{1/7}$). In [26], the same result was found for Pb(l) spreading on pre-wet Cu(100) but kinetics on the pre-wet surface were significantly more rapid. The molecular kinetic model for describing wetting and spreading involves a friction or resistance parameter ζ [6]. Drops spread significantly slower on bare Cu(100), which implies larger ζ than for spreading on pre-wet surfaces. Thus, dissipation due to reactive precursor film formation can be interpreted as higher friction between the spreading drop and the substrate.

From [26] and results presented here, it is clear that reactive precursor film formation slows drop kinetics. In [26], it was reported that the precursor foot advanced somewhat faster on a frozen Cu(100) lattice than on a mobile lattice. However, this result was obtained using spherical starting states and subsequent analysis has

shown that this is only true during the early *t* transition from a sphere to a hemispherical cap. Analysis after this transition regime revealed somewhat *faster* kinetics when the precursor film is permitted to alloy with the Cu surface. Utilizing a rigid substrate lattice provides a way to turn off reactions with the substrate but also introduces an artificial nature to the interaction between liquid and solid. As such, we do not pursue the difference between these two cases further but emphasize that this is an important clarification to earlier results. This does not alter the primary conclusions of [26]: that precursor film kinetics limit drop kinetics on Cu(100) and that slow precursor kinetics are associated with a surface alloying reaction between the precursor film and the Cu surface.

4. Conclusions

MD simulations of wetting in metal systems were performed for AgCu, an eutectic binary, and PbCu, an immiscible binary. Bulk binary phase diagram properties were directly reflected in interfacial properties as exhibited by wetting behavior. The eutectic AgCu system exhibited significant substrate (Cu) dissolution during spreading, resulting in a non-planar solid/liquid interface. Dissolution kinetics dictate spreading kinetics for AgCu. Since dissolution kinetics were the same for Ag(l) on Cu(100) as for Ag(l) on Cu(111), spreading kinetics were very similar on the two crystal surfaces. Spreading of Pb(l) on Cu(100) and Cu(111) occurred virtually in the absence of substrate dissolution and the solid/liquid interface remained planar. For wetting on both crystal surfaces, a precursor film was seen to emerge from a partially wetting drop and advance diffusively across the Cu surface. While a precursor film is observed on both crystal surfaces, kinetics of precursor film advancement are significantly faster for Pb(l) on Cu(111) compared to Cu(100). Rapid kinetics on Cu(111) are associated with advancement of an overlayer and slower kinetics on Cu(100) with advancement of an alloy layer. Slow precursor kinetics on Cu(100) control drop kinetics but the latter are still well described by the molecular kinetic model of wetting and spreading.

Simulation results generally demonstrate that atomistic modeling is capable of investigating reactive wetting in realistic metal systems exhibiting significantly different chemistry. Results will hopefully assist in formulation of more refined models addressing reactive wetting for length and time scales similar to experiment and engineering processes.

Sandia is a multiprogram laboratory operated by Sandia Corporation, a Lockheed Martin Company, for the United States Department of Energy's National Nuclear Security Administration under Contract DE-AC04-94AL85000.

References

1. T. YOUNG, *Philos. Trans. R. Soc. London* **95** (1805) 65.
2. W. P. HARDY, *Philos. Mag.* **38** (1919) 49.
3. D. BEAGLEHOLE, *J. Phys. Chem.* **93** (1989) 893.
4. F. HESLOT, N. FRAYSSE and A. M. CAZABAT, *Nature (London)* **338** (1989) 640; F. HESLOT, A. M. CAZABAT and P. LEVINSON, *Phys. Rev. Lett.* **62** (1989) 1286; F. HESLOT, A. M. CAZABAT, P. LEVINSON and N. FRAYSSE, *ibid.* **65** (1990) 599.
5. M. J. DE RUIJTER, M. CHARLOT, M. VOUÉ and J. D. CONINCK, *Langmuir* **16** (2000) 2363.
6. T. D. BLAKE and J. M. HAYNES, *J. Colloid Interf. Sci.* **30** (1969) 421.
7. B. W. CHERRY and C. M. HOLMES, *ibid.* **29** (1969) 174.
8. L. H. TANNER, *J. Phys. D: App. Phys.* **12** (1979) 1473.
9. P. G. DE GENNES, *Rev. Mod. Phys.* **57** (1985) 827.
10. S. F. BURLATSKY, G. OSHANIN, A. M. CAZABAT and M. MOREAU, *Phys. Rev. Lett.* **76** (1996) 86.
11. M. VOUÉ and J. D. CONINCK, *Acta Mater.* **48** (2000) 4405.
12. D. R. HEINE, G. S. GREST and E. B. WEBB III, *Phys. Rev. E* **68** (2003) 061603.
13. K. LANDRY and N. EUSTATHOPOULOS, *Acta Mater.* **44** (1996) 3923.
14. C. IWAMOTO and S. TANAKA, *ibid.* **50** (2002) 749.
15. F. G. YOST, P. A. SACKINGER and E. J. O'TOOLE, *ibid.* **46** (1998) 2329.
16. R. ASTHANA and N. SOBCZAK, *JOM-e* **52** (2000) 1, http://www.tms.org/pubs/journals/JOM/0001/Asthana/Asthana-0001.html.
17. D. R. MILNER, *British Welding Jnl.* **90** (1958).
18. A. MORTENSEN, B. DREVET and N. EUSTATHOPOULOS, *Scripta Mater.* **36** (1997) 645.
19. F. G. YOST, *ibid.* **42** (2000) 801.
20. O. DEZELLUS, F. HODAJ and N. EUSTATHOPOULOS, *Acta Mater.* **50** (2002) 4741.
21. J. A. WARREN, W. J. BOETTINGER and A. R. ROOSEN, *ibid.* **46** (1998) 3247.
22. R. GE, P. C. CLAPP and J. A. RIFKEN, *Surf. Sci.* **426** (1999) L413.
23. T. SWILER, *Acta Mater.* **48** (2000) 4775.
24. J. MOON *et al.*, *Comp. Mat. Sci.* **25** (2002) 503.
25. E. B. WEBB III and G. S. GREST, *Scripta Mater.* **47** (2002) 393.
26. E. B. WEBB III, G. S. GREST and D. R. HEINE, *Phys. Rev. Lett.* **91**, (2003) 236102.
27. E. B. WEBB III, G. S. GREST, D. R. HEINE and J. J. HOYT, *Acta Mater.* submitted.
28. M. S. DAW and M. I. BASKES, *Phys. Rev. B* **29** (1984) 6443.
29. S. M. FOILES, M. I. BASKES and M. S. DAW, *ibid.* **33** (1986) 7983.
30. M. S. DAW, S. M. FOILES and M. I. BASKES, *Mater. Sci. Rep.* **9** (1993) 251.
31. J. J. HOYT, J. W. GARVIN, E. B. WEBB III and M. ASTA, *Modell. Simul. Mater. Sci. Eng.* **11** (2003) 287.
32. H. S. LIM, C. K. ONG and F. ERCOLESSI, *Surf. Sci.* **269/270** (1992) 1109.
33. M. P. ALLEN and D. J. TILDESLEY, "Computer Simulation of Liquids" (Clarendon, Oxford, 1987).
34. F. G. YOST and E. J. O'TOOLE, *Acta Mater.* **46** (1998) 5143.
35. N. EUSTATHOPOULOS, *ibid.* **46** (1998) 2319.
36. R. VOITOVITCH, A. MORTENSEN, F. HODAJ and N. EUSTATHOPOULOS, *ibid.* **47** (1999) 1117.
37. Graphics are rendered using the code Raster3D. E. A. MERRITT and D. J. BACON, *Meth. in Enzymol.* **277** (1997) 505.

Received 31 March
and accepted 20 October 2004